Diradical Generation via Relayed Proton-Coupled Electron Transfer

Qianqian Shi[a], Zhipeng Pei[b], Jinshuai Song[a], Shi-Jun Li[a], Donghui Wei,[a,*] Michelle L. Coote,[b,*] Yu Lan[a,*]

[a] *Green Catalysis Center, and College of Chemistry, Zhengzhou University, Zhengzhou, Henan 450001, China.*

[b] *Research School of Chemistry, Australian National University, Canberra, ACT 2601, Australia;*

[*]Emails: donghuiwei@zzu.edu.cn (Donghui Wei), michelle.coote@anu.edu.au (Michelle L. Coote), lanyu@cqu.edu.cn(Yu Lan)

ABSTRACT: Diradical generation followed by radical-radical cross-coupling is a powerful synthetic tool, but its detailed mechanism has yet to be established. Herein, we proposed and confirmed a new model named relayed proton-coupled electron transfer (relayed--PCET) for diradical generation, which could open a door for new radical-radical cross-coupling reactions. Quantum mechanics calculations were performed on a selected carbene-mediated diradical cross-coupling reaction model and a designed model, and the exact electronic structural changes during the radical processes have been observed for the first time.

1. INTRODUCTION

Once dismissed as unselective and suitable only for initiating polymerization, in recent years there has been enormous progress towards taming free radicals for applications in target synthesis[1-5]. Critical to their success, has been the development of powerful but highly selective methods for radical generation, particularly using photochemistry[6-11], electrochemistry[12-14], organic super-electron donors[15], and transition metal catalysis[16-18]. Nonetheless, the discovery of new strategies of radical generation[19-25] particularly under light-free, electricity-free, metal-free conditions, remains crucial. Organocatalysis, particularly involving N-heterocyclic carbenes (NHCs), shows promise approach for realizing radical generation and radical-radical cross-coupling[26-35]. However, to develop this chemistry, a greater understanding of how they mediate electron transfer is critical.

NHC-catalyzed radical reactions involving single electron transfer (SET) processes have been significantly developed experimentally, but the detailed mechanism of the radical generation process remains uncertain. Since Studer and co-workers reported that a SET reaction can happen between the Breslow intermediate and the oxidant 2,2,6,6-tetramethylpiperidine 1-oxyl (TEMPO) in 2008[36], a series of radical-radical cross-coupling reactions involving C–C bond formations through the recombination of *in situ* generated radicals have been reported, and this has greatly promoted the development of NHC catalysis. Notably, Chi and co-workers reported an excellent example of carbene catalyzed reductive coupling of nitrobenzyl bromides and activated ketones[28]. Subsequently, Ohmiya and co-workers contributed a series of NHC-catalyzed cross-coupling reactions of aldehydes and N-hydroxyphthalimide (NHPI) esters[32-35]. Recently, Hong and co-workers reported the NHC catalyzed cross-coupling reaction between aldehydes and Katritzky pyridinium salts[37]. The stepwise SET process was commonly proposed in these experimental reports. However, other pathways for diradical generation from the non-radical substrates should be also possible in theory.

Herein, we use theory to uncover a new model for NHC-catalyzed radical reactions, in which a diradical is formed from two non-radical substrates by single-electron transfer in concert with proton transfer. This is reminiscent of standard proton-coupled electron transfer (PCET)[38-41] except that it is effectively a three-component system in which one non-radical component receives an electron from another non-radical source, while it simultaneously transfers its proton to a weakly coordinated base (**Scheme 1a**). Because the electron donor D (which we call here the substrate Sub) and acceptor A (which we call the oxidant Ox) are both initially non-radical species, PCET in this case is accompanied by a shell change, thereby forming an open-shell singlet diradical species that can then undergo radical recombination to afford the cross-coupled product. The overall process, which we refer to as relayed-PCET is shown in **Scheme 1**. In the first stage of relayed-PCET depicted in **Scheme 1b**, the driving force of the electron transfer from Sub to Ox is the proton transfer from Sub to the base. In the second stage the open-shell singlet intermediate undergoes radical-radical recombination to construct a new C–C bond.

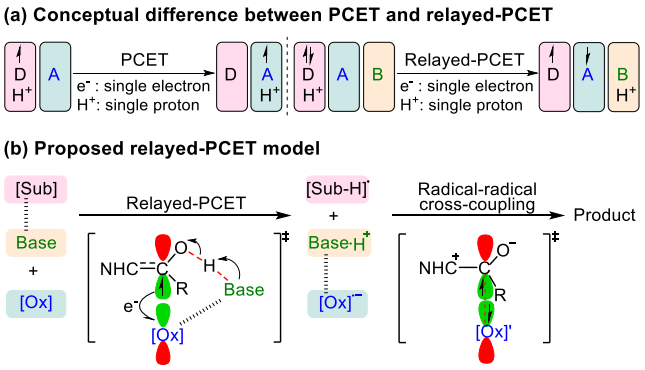

Scheme 1. (a) Conceptual Difference between Standard PCET and Relayed-PCET. In Relayed-PCET, D and A Are Both Initially Non-Radical Species, and B Is a Base Remotely Coordinated to A. (b) Proposed Relayed-PCET Mechanism and Its Use in Cross-Coupling. Here [Sub] Corresponds to the Donor D in Part (a), [Ox] Corresponds to the Acceptor A, and Both Are Initially Non-Radical Species.

While radical reactions involving the transformation from the closed-shell molecules to the radicals are well known[42-44], this relayed-PCET model is distinctive in that it requires the

presence of a base to facilitate the proton transfer component. Although the concept of a relayed proton in PCET reactions has been significantly discussed in the previous references,[40,45-51] to the best of our knowledge, a model for the simultaneous generation of diradicals from the closed-shell molecules has not yet been confirmed in these reactions.

For validating our model, we first selected the carbene-catalyzed oxidative radical-radical cross-coupling reaction between **R1** and **R2** depicted in **Scheme 2** as a case study[33]. Based on our previous experience[52-55], we then designed a new diradical generation model employing TEMPOH as proton and electron donor based on the relayed-PCET concept, to demonstrate its broader applicability. In these NHC-promoted radical reactions, nucleophilic attack of the **NHC** to the aldehyde forms the Breslow intermediate, which reacts with oxidant and base to form two radicals that undergo diradical cross-coupling to generate the final product. However, it remains unclear as to whether the deprotonation by base and electron transfer to oxidant are stepwise or concerted. To address this question, quantum mechanics calculations were performed on a carbene-mediated diradical cross-coupling model, and the accompanying changes in electronic structure during the radical processes have been reported for the first time, revealing this its underlying relayed-PCET mechanism.

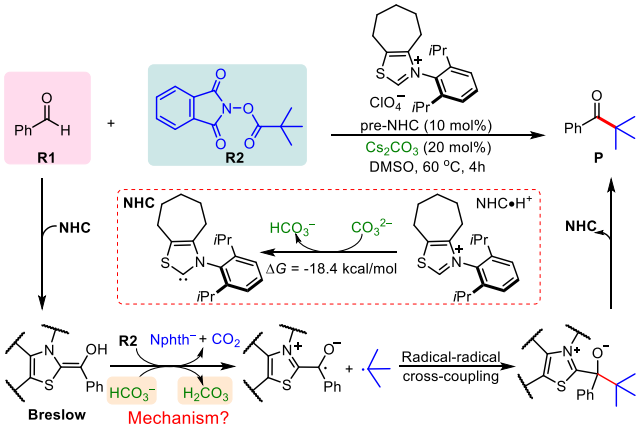

Scheme 2. Case Study in the Present Work: NHC-Catalyzed Oxidative Radical-Radical Cross-Coupling[33]. The Content in Red Box Shows Gibbs Free Energy Change of the Transformation from NHC•H$^+$ to **NHC**.

2. COMPUTATIONAL DETAILS

The geometries of the stationary points and frequencies (1 atm, 298 K) were optimized using M06-2X[56] functional with 6-31G(d,p) basis set in dimethyl sulfoxide (DMSO) solvent using the integral equation formulation of the polarizable continuum model (IEF-PCM)[57,58]. The free energy was obtained at the M06-2X/6-311++G(d,p)/IEF-PCM(DMSO)//M06-2X/6-31G(d,p)/IEF-PCM(DMSO) level using the Gaussian16 program[59]. Other DFT methods and basis sets were also employed to test and ensure the reliability of the selected computational method, and the computed results were summarized in **Table S1** of Supporting information (SI). The minimum energy crossing point (MECP) has been located using the program of sobMECP[60], which based on the work of Harvey[61] and Robb[62].

Since explicit solvents are often important for organic reactions involving proton transfer[63], we also constructed an explicit solvent model containing 50 DMSO solvent molecules for the open-shell transition state ^{os}**TSm** of case study 2 (vide infra). The explicit solvent model was constructed by using Packmol software[64], and studied with ONIOM(M06-2X/6-311++G(d,p):UFF)//ONIOM(M06-2X/6-31G(d,p):UFF) computations. All reaction partners and two DMSO solvent molecules in included in the quantum mechanical region, were carried out in the Gaussian program. The calculated results demonstrate that the difference between the energy barriers of the explicit solvent model and the implicit model is only 1.7 kcal/mol (See **Table S2** of SI), indicating that the selected computational method should be reliable. In a similar vein, we also considered the effect of adding Cs^+ metal cation coordinated with solvent DMSO (See **Table S3** of SI) for PCET steps of case studies 1 and 2. The computed energy barriers are relatively unaffected by the presence or absence of Cs^+, thus supporting the computational models and results.

Finally, it should be noted that for simplicity we neglect nuclear quantum effects, which are known to be important in PCET reactions[65,66], and, while tunneling complicates the representation of the reaction coordinate[67-71], it is not expected to affect the qualitative conclusions.

3. RESULTS AND DISCUSSION

Case Study 1: NHC-Catalyzed Cross-Coupling. Initially we studied the NHC-catalyzed oxidative radical-radical cross-coupling reaction in **Scheme 2**.[33] The full system with the 2,6-diisopropylphenyl substituent and the cycloheptyl ring was computed in the energy profiles. Initially, NHC•H$^+$ of the pre-NHC can be deprotonated by base CO_3^{2-}, in turn obtained from the dissociation of additive Cs_2CO_3. This affords the base HCO_3^- and NHC catalyst with a Gibbs free energy change of −18.4 kcal/mol (**Scheme 2**). The free energy profile of the most energetically favorable pathway for the selected NHC-catalyzed reaction depicted in **Figure 1**.

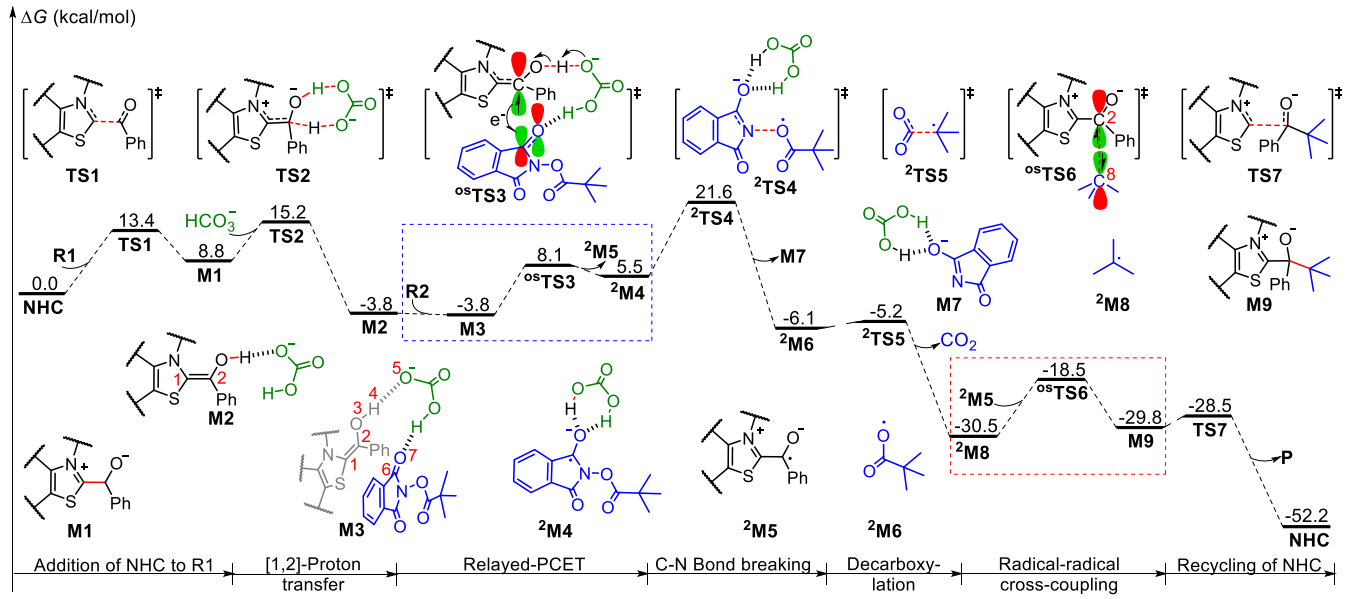

Figure 1. Gibbs free energy profile of the relayed-PCET pathway for the model reaction[33]. The contents in the blue and red boxes represent the relayed-PCET and radical-radical cross-coupling processes, respectively.

As shown in **Figure 1**, a Breslow intermediate involved in **M2** can be formed through nucleophilic addition and base assisted [1,2]-proton transfer transition states **TS1** ($\Delta G^{\ddagger}$ = 13.4 kcal/mol) and **TS2** ($\Delta G^{\ddagger}$ = 6.4 kcal/mol). This then reacts with **R2** to form the three-component complex **M3**. Formation of this complex is promoted by a π…π stacking interaction (~3.50 Å, **Figure 2**) between the donor and acceptor, which also provides the π orbital overlap necessary for the subsequent electron transfer. Consistent with previous reports[72,73], this π…π stacking interaction helps to facilitate the electron transfer. These favorable interactions compensate the entropy lost upon complex formation such that, even at 60 °C, the overall equilibrium constant for formation of **M3** from the three isolated components (*i.e.*, **Breslow**, **R2**, and HCO_3^-, **Scheme S2** of SI) is 5.7 × 10^{-2} M^{-2}, and its estimated concentration associated with the literature experimental conditions[33] is 2.7 × 10^{-3} M.

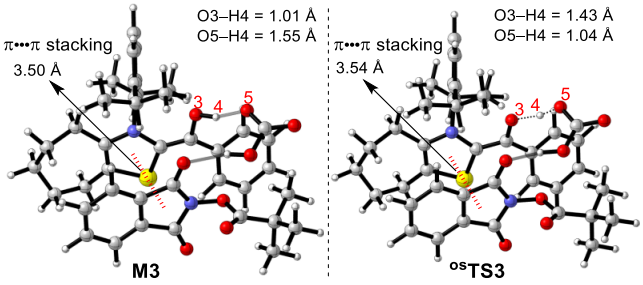

Figure 2. Optimized structures of intermediate **M3** and **^{os}TS3**. Yellow, blue, red, gray, and white balls represent S, N, O, C, and H atoms, respectively, and the same settings were used as follows.

From **M3**, we located a PCET pathway through a concerted open-shell singlet transition state **^{os}TS3** ($\Delta G^{\ddagger}_{\text{relayed-PCET}}$ = 11.9 kcal/mol) to generate radicals **^{2}M4** and **^{2}M5**. This pathway can be compared with the alternative stepwise deprotonation and SET pathway from the same 3-component complex **M3** (See **Figure 3**). In the stepwise process, deprotonation occurs via transition state **TS8** with an energy barrier of 5.1 kcal/mol. The two radicals **^{2}M4** and **^{2}M5** can then be generated via an **MECP**, which is the point at which the open-shell singlet and triplet are degenerate (**Figure 3**). As a non-stationary point, the free energy of **MECP** is difficult to determine, but we can compare the 0 K non-zero-point corrected energies of the (stepwise) **MECP** and (concerted) open-shell singlet transition state as both are unimolecular reactions ultimately originating from **M3**. The **MECP** is 19.2 kcal/mol higher than that of intermediate **M3**, while the concerted **^{os}TS3** is only 12.8 kcal/mol above **M3** (which is close to its free energy barrier of 11.9 kcal/mol). In other words, the stepwise proton transfer and SET (PT-ET) pathway is 6.4 kcal/mol higher than the energy of the alternative concerted transition state, which in turn is a good approximation to their free energy differences. In addition, the Gibbs free energy change for the first SET step of the stepwise SET and proton transfer (ET-PT) pathway is also high (24.2 kcal/mol, **Scheme S3** of SI), so this stepwise pathway can also be excluded. Therefore, the relayed-PCET process is more energetically favorable than the stepwise pathway.

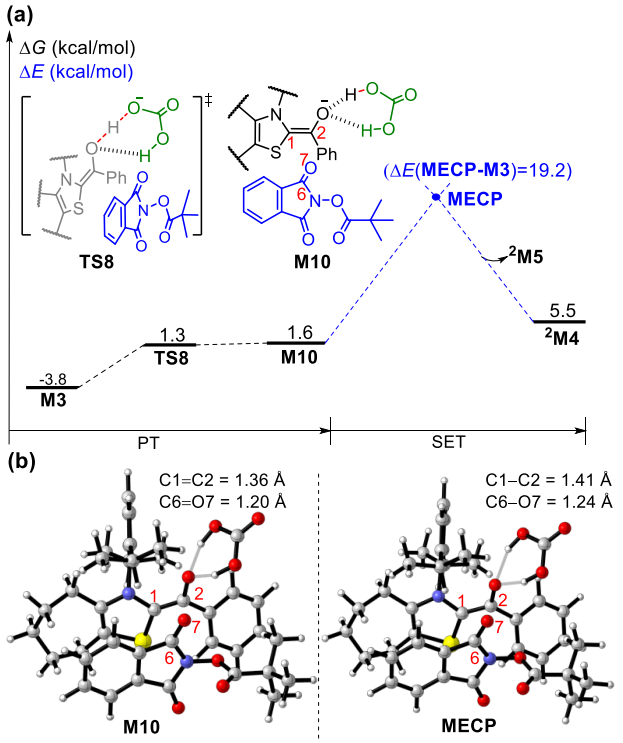

Figure 3. (a) Energy profile of the possible stepwise PT-ET pathway. (b) Optimized structures of intermediate **M10** and **MECP** highlighting the increase in the C1=C2 bond length of the donor and C6=O7 bond length of the electron acceptor.

Returning to the relayed-PCET mechanism in **Figure 1**, after the electron transfer step, ^{2}**M4** undergoes N-O bond activation via a doublet transition state ^{2}**TS4** ($\Delta G^{\ddagger}$ = 16.1 kcal/mol) and then a decarboxylation occurs via transition state ^{2}**TS5** ($\Delta G^{\ddagger}$ = 0.9 kcal/mol). The energy barrier of the decarboxylation with the presence of **M7** via transition state ^{2}**TS5′** (**Figure S3** of SI) is calculated to be 2.4 kcal/mol without the zero-point and thermal corrections, and the corresponding free energy difference is negative (–0.8 kcal/mol), indicating that the process should be barrier-less with the presence of **M7**. Finally, the recombination of two radical intermediates ^{2}**M8** and ^{2}**M5** proceeds via an open-shell singlet transition state ^{os}**TS6** ($\Delta G^{\ddagger}$ = 12.0 kcal/mol), which is followed by the dissociation of the **NHC** via transition state **TS7** ($\Delta G^{\ddagger}$ = 1.3 kcal/mol). The total energy and Gibbs free differences between the open-shell singlet and triplet diradical intermediates ^{os}**M9-F** and ^{3}**M9-F** (*i.e.*, the cross-coupling precursor between ^{2}**M5** and ^{2}**M8**) are 0.7 and 0.1 kcal/mol (**Figure S4** of SI), respectively, indicating that the two radicals could be smoothly transformed to the open-shell singlet. Moreover, we have additionally considered and investigated the possible self-coupling pathway between two ^{2}**M5** intermediates. The calculated results show that the relative Gibbs free energy of the self-coupling product **M5′** is 52.9 kcal/mol higher than that of the two ^{2}**M5** intermediates (**Figure S5** of SI), indicating that this pathway can be safely excluded.

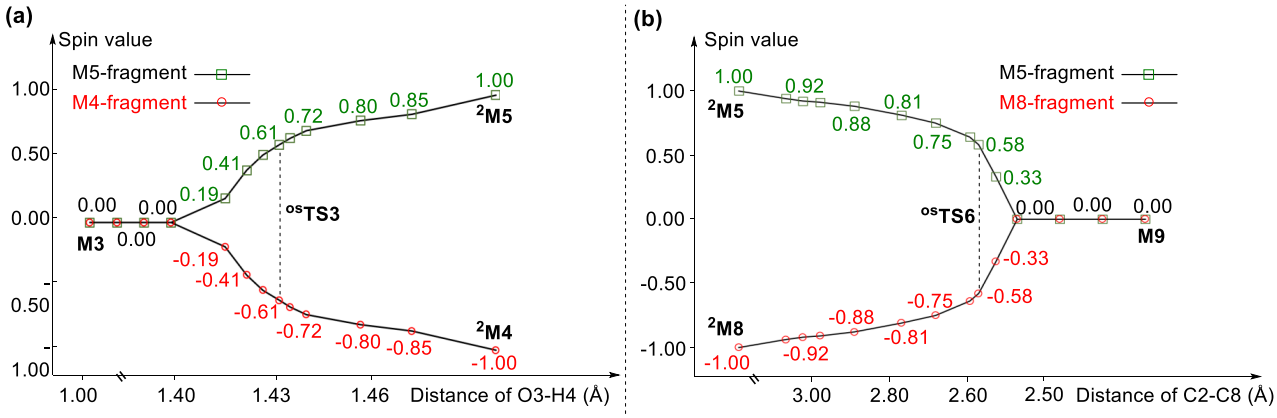

Figure 4. (a) Spin value changes of the M5-fragment and M4-fragment in the selected structures along the IRC results of open-shell singlet transition state ^{os}**TS3** and **M3**. (b) Spin value changes of the M5-fragment and M8-fragment in the selected structures along the IRC results of open-shell singlet transition state ^{os}**TS6** and **M9**.

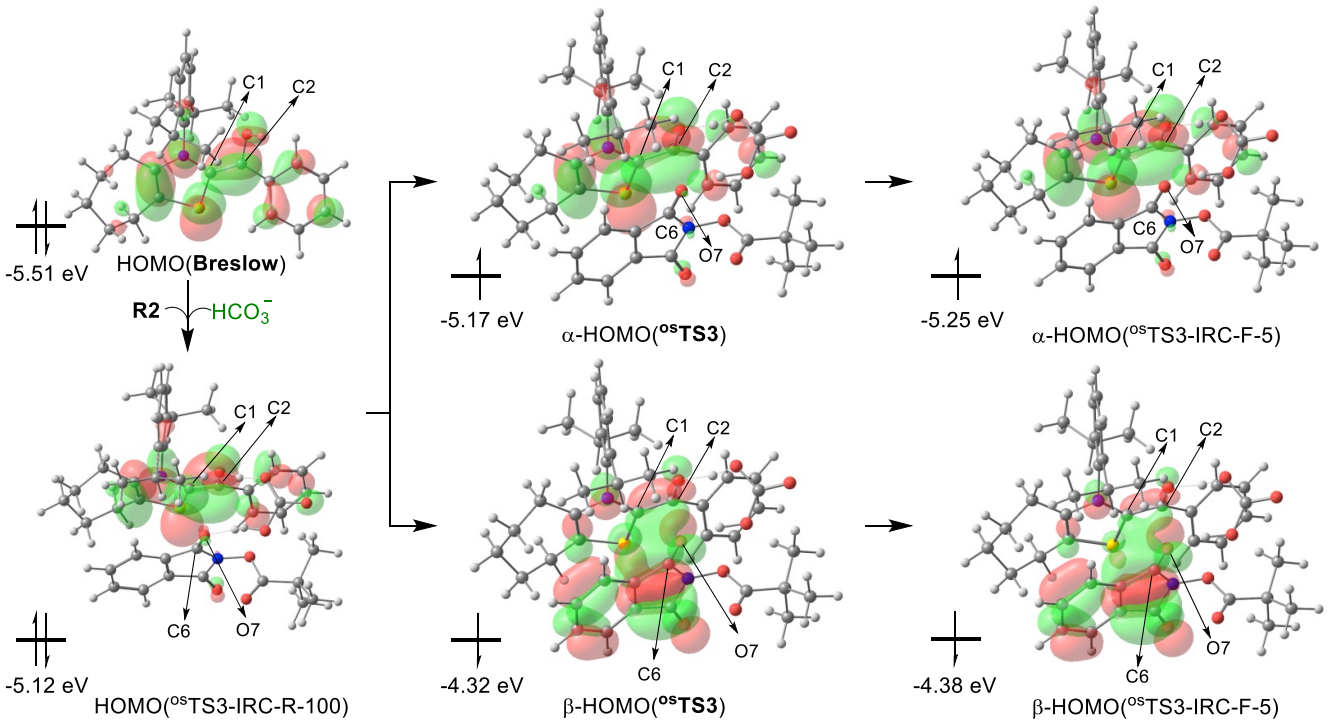

Figure 5. FMO overlap/interaction pictures of the selected structures along the IRC results of open-shell singlet transition state **^{os}TS3**.

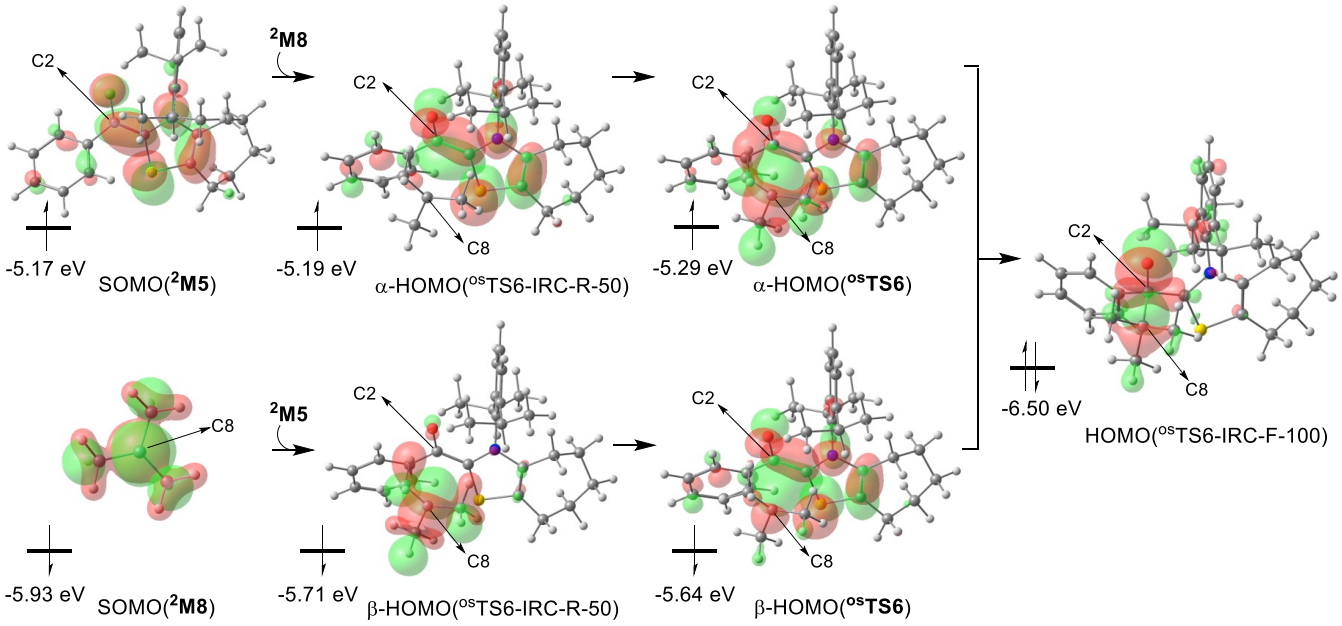

Figure 6. FMO overlap/interaction pictures of the selected structures along the IRC results of open-shell singlet transition state **^{os}TS6**, **^{2}M5**, and **^{2}M8**.

To further investigate the nature of the diradical generation and combination of the two single electrons involved in the selected radical-radical cross-coupling reaction, we have tracked the spin population (spin) and frontier molecular orbital (FMO) overlap/interaction changes along the intrinsic reaction coordinate (IRC) results for the open-shell singlet transition states **^{os}TS3** and **^{os}TS6**. It should be noted that the spin values of base HCO_3^- are less than 0.01 in these structures. **Figure 4** show the spin changes of the two fragments involved in the selected structures along with the IRC coordinates of open-shell singlet transition states **^{os}TS3** and **^{os}TS6**, indicating that a chemical change (*i.e.*, base-assisted proton transfer or C-C bond formation) generally occurs along with the electron transfer (or diradical recombination).

As shown in **Figure 5**, one electron of HOMO(**Breslow**) remains in the same MO, so the α-HOMO is similar to that of HOMO(**Breslow**), while the other electron of HOMO(**Breslow**) is transferred to the oxidant fragment depicted in the β-HOMO pictures. As shown in **Figure 6**, the

two SOMOs of the two radicals overlap to form the C-C bond, and their energies become more similar along the recombination reaction, before finally becoming degenerate and mixing to form the HOMO of **M9**. Furthermore, **Figures 5** and **6** indicate that the single electron transfer and radical-radical recombination involves the π orbital overlap between the two parts.

Finally, we can also understand the role of the base in frontier molecular orbital (FMO) theory terms. As shown in **Figure 7**, the corresponding energy gap between the HOMO(**Breslow**) and LUMO(**R2**) is 4.01 eV, which is further reduced to 3.62 eV in the presence of base HCO_3^-, indicating the electron transfer can be promoted by the base. In addition, the electron transfer between HOMO(**R2**) and LUMO(**Breslow**) is difficult due to the large energy gap between them.

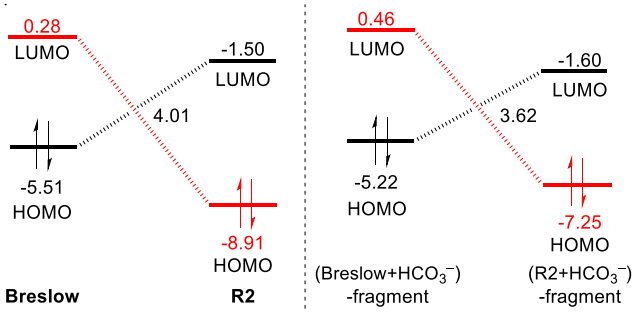

Figure 7. The energy gaps (Unit: eV) of FMOs of **Breslow** and **R2** with or without the presence of a base. The structure fragments were abstracted from the optimized intermediate **M3**.

Case Study 2: Oxidation of TEMPOH by Relayed-PCET. In order to demonstrate the generality of relayed-PCET, the model reaction between TEMPOH (**R3**) and **R2** depicted in **Figure 8** with the presence of base HCO_3^- was also studied. As shown in **Figure 8**, the relayed-PCET process occurs through an open-shell singlet transition state **^{os}TSm** ($\Delta G^{\ddagger}$ = 26.6 kcal/mol), which would lead to the formation of two radical intermediates TEMPO and **^{2}M4**. As shown in **Scheme 3**, the Gibbs free energy changes for the stepwise pathways (*i.e.*, 43.7 and 34.9 kcal/mol) are extremely high, so we can safely exclude the stepwise pathways.

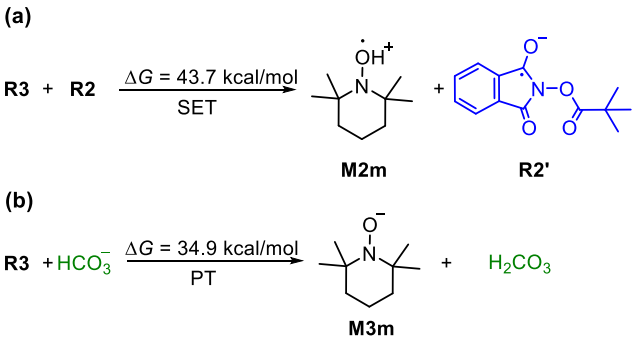

Scheme 3. Gibbs Free Energy Change for the First Step in the Stepwise (a) ET-PT and (b) PT-ET Pathways of Case Study 2.

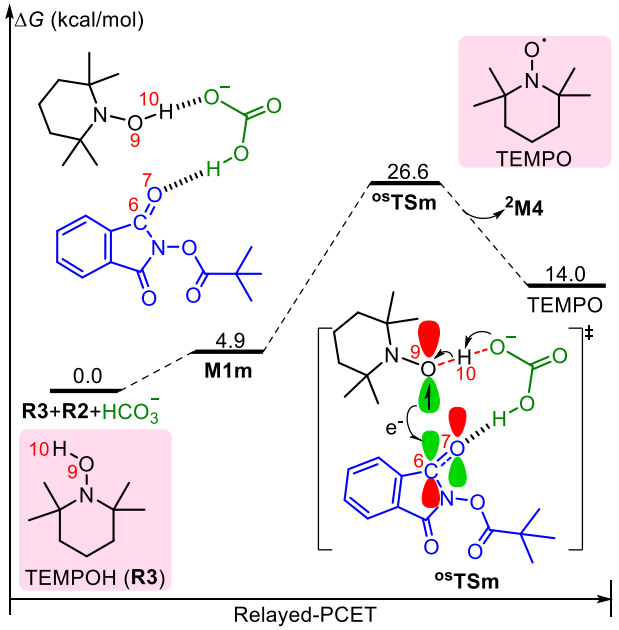

Figure 8. Energy profile of the relayed-PCET pathway of TEMPOH (**R3**) model.

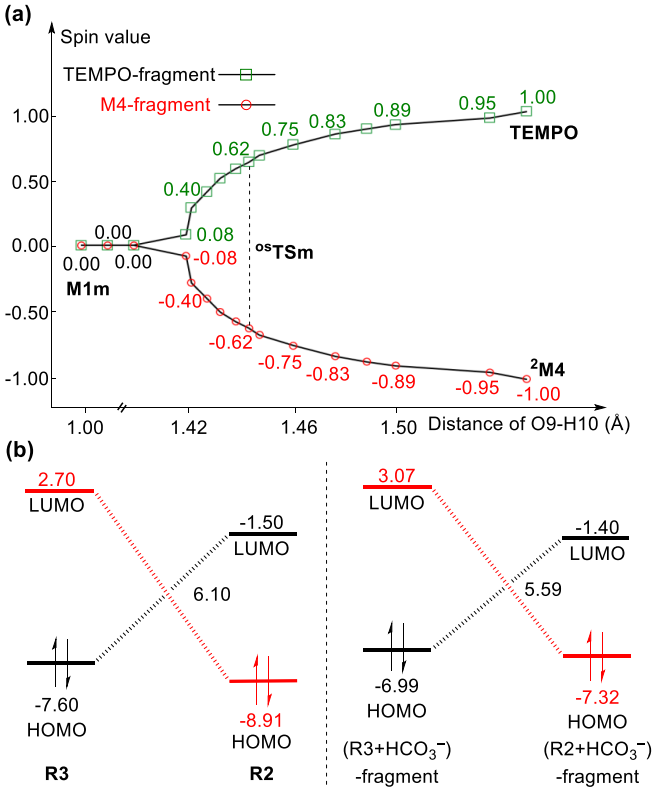

Figure 9. (a) Spin value changes of the TEMPO-fragment and M4-fragment in the selected structures along the IRC results of open-shell singlet transition state **^{os}TSm** and **M1m**. (b) The energy gaps (Unit: eV) of FMOs of **R3** and **R2** with or without the presence of a base. The structure fragments were abstracted from the optimized intermediate **M1m**.

The spin population changes of the TEMPO-fragment and M4-fragment in the selected IRC results of open-shell singlet transition state ^{os}**TSm** are shown in **Figure 9a**. It can be seen that the total spin on each fragment changes from 0 to ±1 as the O-H distance is increased, which is similar with the above relayed-PCET process via open-shell singlet transition state ^{os}**TS3**. Moreover, the corresponding energy gap between HOMO(**R3**) and LUMO(**R2**) depicted in **Figure 9b** could be reduced from 6.10 eV to 5.59 eV in the presence of base HCO_3^- to further promote the electron transfer. The FMO overlap/interaction pictures are shown in the right of **Figure 10**, which shows that the single electron transfer also occurs through the π orbital overlap between the two fragments and the other one keeps in the same orbital. Therefore, these obtained insights could be valuable for the rational design of new a family of radical reactions according to the novel relayed-PCET model.

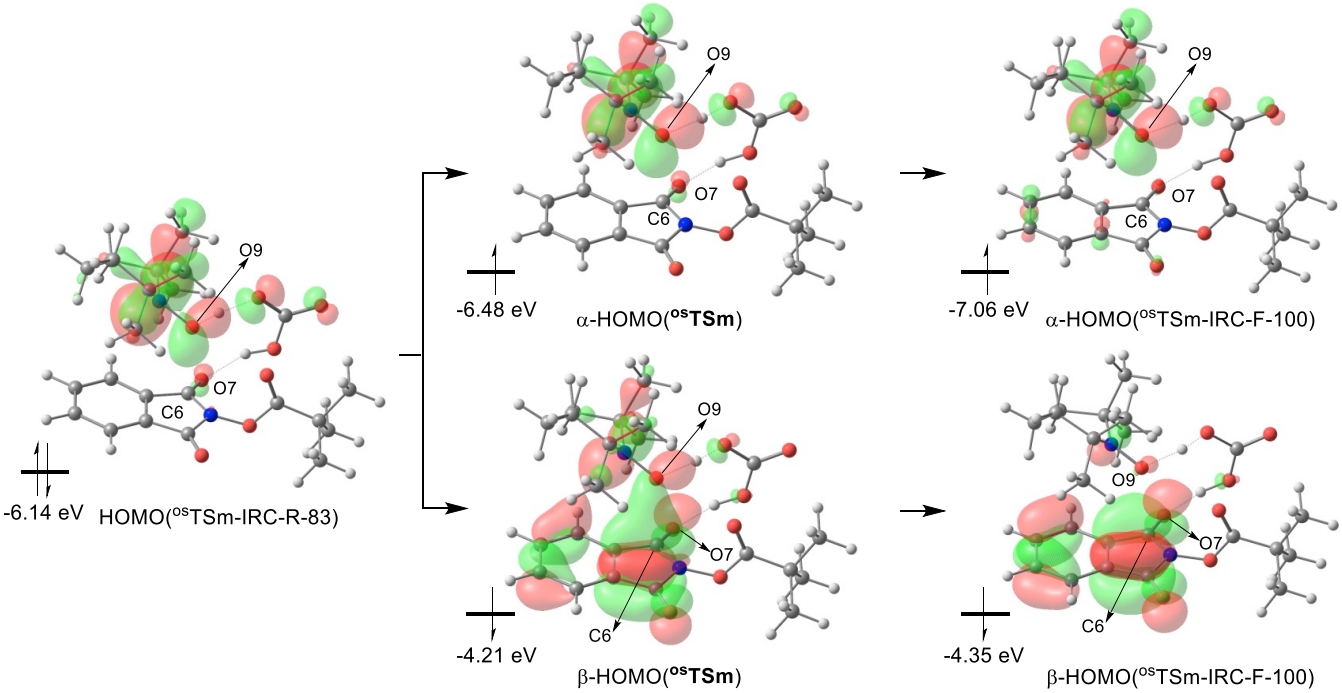

Figure 10. FMO overlap/interaction pictures of the selected structures along the IRC results of open-shell singlet transition state ^{os}**TSm**.

3. CONCLUSION

In summary, the nature of diradical generation based on relayed-PCET model has been scrutinized using quantum mechanics simulations. This work provides a case study to explore the concerted electron transfer and chemical change using various theoretical analyses, including monitoring the changes in spin population and FMO overlap along the IRCs of the novel open-shell singlet transition states. FMO overlap/interaction pictures prove that π orbital overlap is critical for affording a channel for electron transfer. The obtained insights are vital for appreciating the effectiveness of organocatalytic radical-radical cross-coupling reactions and should also be valuable for examining possible pathways for other radical-radical reactions that involve diradical generations and radical-radical cross-couplings.

ASSOCIATED CONTENT

Supporting Information

The Supporting Information is available free of charge on the ACS Publications website.

Computational Details, Tests of the Influence of Explicit Solvent in relayed-PCET Process, Other Possible Pathways of relayed-PCET and Deprotonation Processes, Relayed-PCET Pathways in the Presence of [Cs], IRC Results of Key Transition States, Cartesian Coordinates and Absolute Energies of the Optimized Structures. (PDF)

AUTHOR INFORMATION

Authors

Qianqian Shi - *Green Catalysis Center, and College of Chemistry, Zhengzhou University, Zhengzhou, Henan 450001, China;*

Zhipeng Pei - *Research School of Chemistry, Australian National University, Canberra, ACT 2601, Australia;*

Jinshuai Song - *Green Catalysis Center, and College of Chemistry, Zhengzhou University, Zhengzhou, Henan 450001, Henan, China;*

Shi-Jun Li - *Green Catalysis Center, and College of Chemistry, Zhengzhou University, Zhengzhou, Henan 450001, Henan, China*

Corresponding Authors

Donghui Wei - *Green Catalysis Center, and College of Chemistry, Zhengzhou University, Zhengzhou, Henan 450001, Henan, China;* Email: donghuiwei@zzu.edu.cn

Michelle L. Coote - *Research School of Chemistry, Australian National University, Canberra, ACT 2601, Australia;* E-mail: michelle.coote@anu.edu.au

Yu Lan - *Green Catalysis Center, and College of Chemistry, Zhengzhou University, Zhengzhou, Henan 450001, China;* Email: lanyu@cqu.edu.cn

Notes

The authors declare no competing financial interest.

ACKNOWLEDGMENT

The authors gratefully thank the financial support from National Natural Science Foundation of China (Nos. 21773214, 21822303, 21772020), Natural Science Foundation for Excellent Young Scientist in Henan Province (No. 212300410083), 111 Project (D20003), Backbone Teacher Project (2020GGJS016), National Supercomputing Center in Zhengzhou. MLC gratefully acknowledges an Australian Research Council Laureate Fellowship (FL170100041). ZP acknowledges helpful discussions with Prof. Gino DiLabio on PCET mechanisms.

REFERENCES

(1) Dong, Z.; MacMillan, D. W. C. Metallaphotoredox-Enabled Deoxygenative Arylation of Alcohols. *Nature* **2021**, *598*, 451-456.
(2) Huang, H.-M.; Bellotti, P.; Glorius, F. Transition Metal-Catalysed Allylic Functionalization Reactions Involving Radicals. *Chem. Soc. Rev.* **2020**, *49*, 6186-6197.
(3) Yi, H.; Zhang, G.; Wang, H.; Huang, Z.; Wang, J.; Singh, A. K.; Lei, A. Recent Advances in Radical C–H Activation/Radical Cross-Coupling. *Chem. Rev.* **2017**, *117*, 9016-9085.
(4) Fu, M.-C.; Shang, R.; Zhao, B.; Wang, B.; Fu, Y. Photocatalytic Decarboxylative Alkylations Mediated by Triphenylphosphine and Sodium Iodide. *Science* **2019**, *363*, 1429-1434.
(5) Sumida, Y.; Ohmiya, H. Direct Excitation Strategy for Radical Generation in Organic Synthesis. *Chem. Soc. Rev.* **2021**, *50*, 6320-6332.
(6) Ahangarpour, M.; Kavianinia, I.; Harris, P. W. R.; Brimble, M. A. Photo-Induced Radical Thiol–Ene Chemistry: A Versatile Toolbox for Peptide-Based Drug Design. *Chem. Soc. Rev.* **2021**, *50*, 898-944.
(7) Bell, J. D.; Murphy, J. A. Recent Advances in Visible Light-Activated Radical Coupling Reactions Triggered by (I) Ruthenium, (Ii) Iridium and (Iii) Organic Photoredox Agents. *Chem. Soc. Rev.* **2021**, *50*, 9540-9685.
(8) Kwon, K.; Simons, R. T.; Nandakumar, M.; Roizen, J. L. Strategies to Generate Nitrogen-Centered Radicals That May Rely on Photoredox Catalysis: Development in Reaction Methodology and Applications in Organic Synthesis. *Chem. Rev.* **2022** *122*, 2353-2428.
(9) Latrache, M.; Hoffmann, N. Photochemical Radical Cyclization Reactions with Imines, Hydrazones, Oximes and Related Compounds. *Chem. Soc. Rev.* **2021**, *50*, 7418-7435.
(10) Shu, C.; Noble, A.; Aggarwal, V. K. Metal-Free Photoinduced C(sp^3)–H Borylation of Alkanes. *Nature* **2020**, *586*, 714-719.
(11) Wang, J.; Fang, W.-H.; Qu, L.-B.; Shen, L.; Maseras, F.; Chen, X. An Expanded Set Model Associated with the Functional Hindrance Dominates the Amide-Directed Distal sp^3 C–H Functionalization. *J. Am. Chem. Soc.* **2021**, *143*, 19406-19416.
(12) Wang, F.; Stahl, S. S. Electrochemical Oxidation of Organic Molecules at Lower Overpotential: Accessing Broader Functional Group Compatibility with Electron−Proton Transfer Mediators. *Acc. Chem. Res.* **2020**, *53*, 561-574.
(13) Wang, Z.; Pan, X.; Li, L.; Fantin, M.; Yan, J.; Wang, Z.; Wang, Z.; Xia, H.; Matyjaszewski, K. Enhancing Mechanically Induced Atrp by Promoting Interfacial Electron Transfer from Piezoelectric Nanoparticles to Cu Catalysts. *Macromolecules* **2017**, *50*, 7940-7948.
(14) Holst, D. E.; Wang, D. J.; Kim, M. J.; Guzei, I. A.; Wickens, Z. K. Aziridine Synthesis by Coupling Amines and Alkenes via an Electrogenerated Dication. *Nature* **2021**, *596*, 74-79.
(15) Murphy, J. A. Discovery and Development of Organic Super-Electron-Donors. *J. Org. Chem.* **2014**, *79*, 3731-3746.
(16) Crossley, S. W. M.; Obradors, C.; Martinez, R. M.; Shenvi, R. A. Mn-, Fe-, and Co-Catalyzed Radical Hydrofunctionalizations of Olefins. *Chem. Rev.* **2016**, *116*, 8912-9000.
(17) Tang, S.; Liu, K.; Liu, C.; Lei, A. Olefinic C–H Functionalization through Radical Alkenylation. *Chem. Soc. Rev.* **2015**, *44*, 1070-1082.
(18) Liu, L.; Aguilera, M. C.; Lee, W.; Youshaw, C. R.; Neidig, M. L.; Gutierrez, O. General Method for Iron-Catalyzed Multicomponent Radical Cascades–Cross-Couplings. *Science* **2021**, *374*, 432-439.
(19) Kurandina, D.; Yadagiri, D.; Rivas, M.; Kavun, A.; Chuentragool, P.; Hayama, K.; Gevorgyan, V. Transition-Metal- and Light-Free Directed Amination of Remote Unactivated C(sp^3)–H Bonds of Alcohols. *J. Am. Chem. Soc.* **2019**, *141*, 8104-8109.
(20) Wang, X.; Studer, A. Iodine(III) Reagents in Radical Chemistry. *Acc. Chem. Res.* **2017**, *50*, 1712-1724.
(21) Kischkewitz, M.; Okamoto, K.; Mück-Lichtenfeld, C.; Studer, A. Radical-Polar Crossover Reactions of Vinylboron Ate Complexes. *Science* **2017**, *355*, 936-938.
(22) Debien, L.; Quiclet-Sire, B.; Zard, S. Z. Allylic Alcohols: Ideal Radical Allylating Agents? *Acc. Chem. Res.* **2015**, *48*, 1237-1253.
(23) Yoshimura, A.; Zhdankin, V. V. Advances in Synthetic Applications of Hypervalent Iodine Compounds. *Chem. Rev.* **2016**, *116*, 3328-3435.
(24) Liu, L.; Ward, R. M.; Schomaker, J. M. Mechanistic Aspects and Synthetic Applications of Radical Additions to Allenes. *Chem. Rev.* **2019**, *119*, 12422-12490.
(25) Lasso, J. D.; Castillo-Pazos, D. J.; Li, C.-J. Green Chemistry Meets Medicinal Chemistry: A Perspective on Modern Metal-Free Late-Stage Functionalization Reactions. *Chem. Soc. Rev.* **2021**, *50*, 10955-10982.
(26) White, N. A.; Rovis, T. Enantioselective N-Heterocyclic Carbene-Catalyzed β-Hydroxylation of Enals Using Nitroarenes: An Atom Transfer Reaction That Proceeds via Single Electron Transfer. *J. Am. Chem. Soc.* **2014**, *136*, 14674-14677.
(27) Zhang, Y.; Du, Y.; Huang, Z.; Xu, J.; Wu, X.; Wang, Y.; Wang, M.; Yang, S.; Webster, R. D.; Chi, Y. R. N-Heterocyclic Carbene-Catalyzed Radical Reactions for Highly Enantioselective β-Hydroxylation of Enals. *J. Am. Chem. Soc.* **2015**, *137*, 2416-2419.
(28) Li, B.-S.; Wang, Y.; Proctor, R. S. J.; Zhang, Y.; Webster, R. D.; Yang, S.; Song, B.; Chi, Y. R. Carbene-Catalysed Reductive Coupling of Nitrobenzyl Bromides and Activated Ketones or Imines via Single-Electron-Transfer Process. *Nat. Commun.* **2016**, *7*, 12933.
(29) Zhao, K.; Enders, D. Merging N-Heterocyclic Carbene Catalysis and Single Electron Transfer: A New Strategy for Asymmetric Transformations. *Angew. Chem. Int. Ed.* **2017**, *56*, 3754-3756.
(30) Song, R.; Chi, Y. R. N-Heterocyclic Carbene Catalyzed Radical Coupling of Aldehydes with Redox-Active Esters. *Angew. Chem. Int. Ed.* **2019**, *58*, 8628-8630.
(31) Dai, L.; Ye, S. Recent Advances in N-Heterocyclic Carbene-Catalyzed Radical Reactions. *Chin. Chem. Lett.* **2021**, *32*, 660-667.
(32) Ishii, T.; Ota, K.; Nagao, K.; Ohmiya, H. N-Heterocyclic Carbene-Catalyzed Radical Relay Enabling Vicinal Alkylacylation of Alkenes. *J. Am. Chem. Soc.* **2019**, *141*, 14073-14077.
(33) Ishii, T.; Kakeno, Y.; Nagao, K.; Ohmiya, H. N-Heterocyclic Carbene-Catalyzed Decarboxylative Alkylation of Aldehydes. *J. Am. Chem. Soc.* **2019**, *141*, 3854-3858.

(34) Matsuki, Y.; Ohnishi, N.; Kakeno, Y.; Takemoto, S.; Ishii, T.; Nagao, K.; Ohmiya, H. Aryl Radical-Mediated N-Heterocyclic Carbene Catalysis. *Nat. Commun.* **2021**, *12*, 3848.
(35) Kakeno, Y.; Kusakabe, M.; Nagao, K.; Ohmiya, H. Direct Synthesis of Dialkyl Ketones from Aliphatic Aldehydes through Radical N-Heterocyclic Carbene Catalysis. *ACS Catal.* **2020**, *10*, 8524-8529.
(36) Guin, J.; De Sarkar, S.; Grimme, S.; Studer, A. Biomimetic Carbene-Catalyzed Oxidations of Aldehydes Using TEMPO. *Angew. Chem. Int. Ed.* **2008**, *47*, 8727-8730.
(37) Kim, I.; Im, H.; Lee, H.; Hong, S. N-Heterocyclic Carbene-Catalyzed Deaminative Cross-Coupling of Aldehydes with Katritzky Pyridinium Salts. *Chem. Sci.* **2020**, *11*, 3192-3197.
(38) Huynh, M. H. V.; Meyer, T. J. Proton-Coupled Electron Transfer. *Chem. Rev.* **2007**, *107*, 5004-5064.
(39) Hammes-Schiffer, S. Theory of Proton-Coupled Electron Transfer in Energy Conversion Processes. *Acc. Chem. Res.* **2009**, *42*, 1881-1889.
(40) Weinberg, D. R.; Gagliardi, C. J.; Hull, J. F.; Murphy, C. F.; Kent, C. A.; Westlake, B. C.; Paul, A.; Ess, D. H.; McCafferty, D. G.; Meyer, T. J. Proton-Coupled Electron Transfer. *Chem. Rev.* **2012**, *112*, 4016-4093.
(41) Hammes-Schiffer, S. Proton-Coupled Electron Transfer: Moving Together and Charging Forward. *J. Am. Chem. Soc.* **2015**, *137*, 8860-8871.
(42) Rüchardt, C.; Gerst, M.; Ebenhoch, J. Uncatalyzed Transfer Hydrogenation and Transfer Hydrogenolysis: Two Novel Types of Hydrogen-Transfer Reactions. *Angew. Chem. Int. Ed.* **1997**, *36*, 1406-1430.
(43) Wagner, P. J.; Zhang, Y.; Puchalski, A. E. Rate Constants for Degenerate Hydrogen Atom Exchange between α-Hydroxy Radicals and Ketones. *J. Phys. Chem.* **1993**, *97*, 13368-13374.
(44) Biondi, C.; Galeazzi, R.; Littarru, G.; Greci, L. Reduction of 1,4-Quinone and Ubiquinones by Hydrogen Atom Transfer under UVA Irradiation. *Free Radic. Res.* **2002**, *36*, 399-404.
(45) Costentin, C.; Robert, M.; Savéant, J.-M.; Tard, C. Inserting a Hydrogen-Bond Relay between Proton Exchanging Sites in Proton-Coupled Electron Transfers. *Angew. Chem. Int. Ed.* **2010**, *49*, 3803-3806.
(46) Verma, S.; Aute, S.; Das, A.; Ghosh, H. N. Proton-Coupled Electron Transfer in a Hydrogen-Bonded Charge-Transfer Complex. *J. Phys. Chem. B* **2016**, *120*, 10780-10785.
(47) Campaña, A. G.; Buñuel, E.; Cuerva, J. M.; Cárdenas, D. J. The Role of Water-Based Hydrogen Atom Wires in Long-Range Electron-Transfer Reactions in Aqueous Media for the Fe^{II}–Fe^{III} Self-Exchange and Related Systems. *Chem. Eur. J.* **2013**, *19*, 16187-16191.
(48) Ren, X.; Wang, X.; Sun, Y.; Chi, X.; Mangel, D.; Wang, H.; Sessler, J. L. Amidinium–Carboxylate Salt Bridge Mediated Proton-Coupled Electron Transfer in a Donor–Acceptor Supramolecular System. *Org. Chem. Front.* **2019**, *6*, 584-590.
(49) Kasanmascheff, M.; Lee, W.; Nick, T. U.; Stubbe, J.; Bennati, M. Radical Transfer in *E. Coli* Ribonucleotide Reductase: A NH_2Y_{731}/R_{411}A-α Mutant Unmasks a New Conformation of the Pathway Residue 731. *Chem. Sci.* **2016**, *7*, 2170-2178.
(50) Roberts, J. A.; Kirby, J. P.; Nocera, D. G. Photoinduced Electron Transfer within a Donor-Acceptor Pair Juxtaposed by a Salt Bridge. *J. Am. Chem. Soc.* **1995**, *117*, 8051-8052.
(51) Kirby, J. P.; Roberts, J. A.; Nocera, D. G. Significant Effect of Salt Bridges on Electron Transfer. *J. Am. Chem. Soc.* **1997**, *119*, 9230-9236.
(52) Wang, G.; Zhang, Q.-C.; Wei, C.; Zhang, Y.; Zhang, L.; Huang, J.; Wei, D.; Fu, Z.; Huang, W. Asymmetric Carbene-Catalyzed Oxidation of Functionalized Aldimines as 1,4-Dipoles. *Angew. Chem. Int. Ed.* **2021**, *60*, 7913-7919.
(53) Wang, J.; Wei, D.; Duan, Z.; Mathey, F. Cleavage of the Inert $C(sp^2)$–Ar σ-Bond of Alkenes by a Spatial Constrained Interaction with Phosphinidene. *J. Am. Chem. Soc.* **2020**, *142*, 20973-20978.
(54) Norcott, P. L.; Hammill, C. L.; Noble, B. B.; Robertson, J. C.; Olding, A.; Bissember, A. C.; Coote, M. L. Tempo–Me: An Electrochemically Activated Methylating Agent. *J. Am. Chem. Soc.* **2019**, *141*, 15450-15455.
(55) Zhong, K.; Shan, C.; Zhu, L.; Liu, S.; Zhang, T.; Liu, F.; Shen, B.; Lan, Y.; Bai, R. Theoretical Study of the Addition of Cu–Carbenes to Acetylenes to Form Chiral Allenes. *J. Am. Chem. Soc.* **2019**, *141*, 5772-5780.
(56) Zhao, Y.; Truhlar, D. G. The M06 Suite of Density Functionals for Main Group Thermochemistry, Thermochemical Kinetics, Noncovalent Interactions, Excited States, and Transition Elements: Two New Functionals and Systematic Testing of Four M06-Class Functionals and 12 Other Functionals. *Theor. Chem. Acc.* **2008**, *120*, 215-241.
(57) Barone, V.; Cossi, M. Quantum Calculation of Molecular Energies and Energy Gradients in Solution by a Conductor Solvent Model. *J. Phys. Chem. A* **1998**, *102*, 1995-2001.
(58) Mennucci, B.; Tomasi, J. Continuum Solvation Models: A New Approach to the Problem of Solute's Charge Distribution and Cavity Boundaries. *J. Phys. Chem.* **1997**, *106*, 5151-5158.
(59) Gaussian 16, Revision A.03, Frisch, M. J.; Trucks, G. W.; Schlegel, H. B. et al. Gaussian, Inc., Wallingford CT, **2016**.
(60) Lu,T. sobMECP program, http://sobereva.com/286 (accessed 2020-10-09).
(61) Harvey, J. N.; Aschi, M.; Schwarz, H.; Koch, W. The Singlet and Triplet States of Phenyl Cation. A Hybrid Approach for Locating Minimum Energy Crossing Points between Non-Interacting Potential Energy Surfaces. *Theor. Chem. Acc.* **1998**, *99*, 95-99.
(62) Bearpark, M. J.; Robb, M. A.; Bernhard Schlegel, H. A Direct Method for the Location of the Lowest Energy Point on a Potential Surface Crossing. *Chem. Phys. Lett.* **1994**, *223*, 269-274.
(63) Winter, A. Making a Bad Calculation. *Nat. Chem.* **2015**, *7*, 473-475.
(64) Martínez, L.; Andrade, R.; Birgin, E. G.; Martínez, J. M. Packmol: A Package for Building Initial Configurations for Molecular Dynamics Simulations. *J. Comput. Chem.* **2009**, *30*, 2157-2164.
(65) Hammes-Schiffer, S.; Stuchebrukhov, A. A. Theory of Coupled Electron and Proton Transfer Reactions. *Chem. Rev.* **2010**, *110*, 6939-6960.
(66) Hammes-Schiffer, S.; Hatcher, E.; Ishikita, H.; Skone, J. H.; Soudackov, A. V. Theoretical Studies of Proton-Coupled Electron Transfer: Models and Concepts Relevant to Bioenergetics. *Coord. Chem. Rev.* **2008**, *252*, 384-394.
(67) Costentin, C.; Savéant, J.-M. Hydrogen and Proton Exchange at Carbon. Imbalanced Transition State and Mechanism Crossover. *Chem. Sci.* **2020**, *11*, 1006-1010.
(68) Borgis, D.; Hynes, J. T. Curve Crossing Formulation for Proton Transfer Reactions in Solution. *J. Phys. Chem.* **1996**, *100*, 1118-1128.
(69) Costentin, C.; Robert, M.; Savéant, J.-M. Concerted Proton−Electron Transfers: Electrochemical and Related Approaches. *Acc. Chem. Res.* **2010**, *43*, 1019-1029.
(70) Costentin, C.; Robert, M.; Savéant, J.-M.; Tard, C. Breaking Bonds with Electrons and Protons. Models and Examples. *Acc. Chem. Res.* **2014**, *47*, 271-280.
(71) Decornez, H.; Hammes-Schiffer, S. Model Proton-Coupled Electron Transfer Reactions in Solution: Predictions of Rates, Mechanisms, and Kinetic Isotope Effects. *J. Phys. Chem. A* **2000**, *104*, 9370-9384.
(72) DiLabio, G. A.; Ingold, K. U. A Theoretical Study of the Iminoxyl/Oxime Self-Exchange Reaction. A Five-Center, Cyclic

Proton-Coupled Electron Transfer. *J. Am. Chem. Soc.* **2005**, *127*, 6693-6699.
(73) DiLabio, G. A.; Johnson, E. R. Lone Pair–π and π–π Interactions Play an Important Role in Proton-Coupled Electron Transfer Reactions. *J. Am. Chem. Soc.* **2007**, *129*, 6199-6203.

TOC Graphic

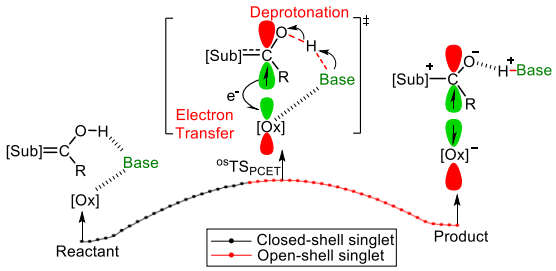
Deprotonation
[Sub]
R
Base
e-
Electron
Transfer
[Ox]
Base
[Sub]
R
[Ox]
[Ox]
Reactant
osTSPCET
Product
Closed-shell singlet
Open-shell singlet